



UPGRADING THE MONARCH OPERATIONAL FORECAST:

UPGRADES IN COUPLING DUST-RADIATION AND SHAPE OF
PARTICLES

BDRC-2023-001

Eleni Karnezi, Emanuele Emili, Sara Basart, Oriol
Jorba, Francesco Benincasa, Miriam Olid, Francesca
Macchia, Gilbert Montané, Alejandro García López,
Carlos Pérez García-Pando*

Barcelona Supercomputing Center, BSC

() Catalan Institution for Research and Advanced Studies, ICREA*

Ernest Werner, Gerardo García-Castrillo

Spanish State Meteorological Agency, AEMET

17 October 2023

TECHNICAL REPORT



BDRC-2023-001

Series: Barcelona Dust Regional Center (BDRC) Technical Report

A full list of BDRC Publications can be found on our website under:

<http://dust.aemet.es/about-us/technical-reports>

© Copyright 2023

Barcelona Dust Regional Center (BDRC)

Plaça d'Eusebi Güell, 1-3 | 08034 Barcelona (Spain)

Library and scientific copyrights belong to BDRC and are reserved in all countries. This publication is not to be reprinted or translated in whole or in part without the written permission of the Technical Director. Appropriate non-commercial use will normally be granted under the condition that reference is made to BDRC. The information within this publication is given in good faith and considered to be true, but BDRC accepts no liability for error, omission and for loss or damage arising from its use.



Summary

This document presents the upgrades that have been introduced in the MONARCH model used for the Barcelona Dust Regional Center (BDRC) operational forecasts. These include a dynamic coupling of dust with radiation, and improvements in the shortwave optical properties of dust by considering size-resolved mineralogical composition and asphericity. For assessing the skills of the upgraded model (v2.1.0) in comparison with the previous operational version (v1.0.0), the model results are evaluated in terms of dust optical depth against AERONET Sun photometers for North Africa, Mediterranean and Middle East (NAMEE) and particulate matter (PM) concentrations over the Iberian Peninsula. The upgraded model version provides in general slightly better forecasts than the former version. The upgraded MONARCH v2.1.0 is used as the new operational version, since June 2023, in the WMO Barcelona Dust Regional Center.

Contents

- 1. MONARCH model..... 2
 - 1.1. Model overview 2
 - 1.2. Model upgrades (MONARCH v2.1.0) 3
 - 1.3. Upgrade in infrastructure 4
- 2. Evaluation strategy 6
 - 2.1 Dust optical depth (DOD) observations: the global AERONET network 6
 - 2.2 PM10 and PM2.5 comparison in Spain 6
- 3. Results 7
 - 3.1 Annual comparison..... 7
 - 3.2 DOD comparison over NAMEE..... 7
 - 3.3 PM₁₀ and PM_{2.5} comparison in Spain 12
- 4. Conclusions 18
- 5. References 19

1. MONARCH model

1.1. Model overview

The Multiscale Online Nonhydrostatic Atmosphere Chemistry model (MONARCH), developed at the Barcelona Supercomputing Center (BSC), is an online meteorology-chemistry model that provides short- and mid-term chemical weather forecasts on both regional and global scales (Pérez et al., 2011; Haustein et al. 2012; Jorba et al. 2012; Spada et al. 2013; Spada et al. 2015; Badia and Jorba 2015; Badia et al. 2017; Di Tomaso et al. 2017; Xian et al., 2019; Klose et al., 2021). MONARCH is based on the online coupling of the meteorological Nonhydrostatic Multiscale Model on the B-grid (NMMB; Janjic and Gall, 2012) developed at the National Centers for Environmental Prediction (NCEP), with a full chemistry module, including gas phase and all aerosol species, developed at the BSC. Therefore, the model is designed to account for the feedback among gases, aerosol particles and meteorology. The aerosol module is enhanced with a data assimilation (DA) system to optimally combine forecasts with observations and improve predictions (Di Tomaso et al. 2017; Di Tomaso et al. 2022; Escribano et al., 2022).

The desert dust module, previously known as NMMB/BSC-Dust (Pérez et al., 2011) that is embedded into the NMMB meteorological core, solves the mass balance equation for dust taking into account the following processes: i) dust generation and uplift by the wind, ii) horizontal and vertical advection, iii) horizontal diffusion and vertical transport by turbulence and convection, iv) dry deposition and gravitational settling, v) wet removal, including in-cloud and below-cloud scavenging. The MONARCH model is the reference model of the WMO Barcelona Dust Regional Center, while the model also contributes to the WMO SDS-WAS regional dust multi-model ensemble, the Copernicus Regional air quality multi-model ensemble, and the ICAP global operational aerosol multi-model ensemble.

The resolution of the model is set to $0.10^\circ \times 0.10^\circ$ covering North Africa, Middle East and Europe (NAMEE, domain) and 40 layers vertically (top of the domain at 50hPa). The Global Forecast System (GFS) at $0.5^\circ \times 0.5^\circ$ and produced at 12UTC by the National Centers for Environmental Prediction (NCEP), is used as initial meteorological conditions and boundary conditions at intervals of 6 h. The simulated dust distributions consist of daily runs of 84-hour forecast length, and the initial state of the dust concentration is defined by the 24-h forecast of the previous-day model run. Only in a ‘cold start’ of the model, concentration is set to zero.

In the previous upgrade (performed in December 2020) with MONARCH v1.0.0, the focus was dust emissions. These were parameterized and tested using two different emission schemes (Ginoux et al., 2001; Kok et al., 2014) as well as different desert dust source functions (Ginoux et al. 2001; 2012). In the end (<https://dust.aemet.es/resources/barcelona-dust-regional-center-technical-report-2020>), the configuration for dust included the use of desert dust source function from the MODIS satellite data (Ginoux et al. 2012) and the simplified emission scheme from Ginoux et al. (2001).

1.2. Model upgrades (MONARCH v2.1.0)

From Klose et al (2021) the representations of dust processes are upgraded allowing simulations with both simplified empirically-based and more complex physics-based parameterizations along with a variety of lower boundary conditions (roughness from different vegetation fraction satellite datasets, potential dust sources). The model includes eight dust size bins; sub-micron particles in bins 1-4 correspond to clay originated particles, while the remaining particles in bins 5-8 to silt (Pérez et al., 2006). The diameter ranges of each bin are specified as follows: 0.2-0.36, 0.36-0.6, 0.6-1.2, 1.2-2.0, 2.0-3.6, 3.6-6.0, 6.0-12.0, and 12.0-20.0 μm from bin 1 to bin 8 respectively. About the Aerosol-Radiation Interaction (ARI), a dynamical coupling of dust with radiation has been implemented, for better representation of dust-radiation interaction (Klose et al., 2021). The previous version (v1.0.0) relied on an aerosol climatology for the ARI effect in the meteorological driver.

For the description of dust aerosols interaction with both the shortwave (SW) and longwave (LW) radiation, the RRTMG (Rapid Radiative Transfer Model for Global Circulation Models, Iacono et al., 2008) radiative transfer model is coupled with the dust module. In the longwave (LW), we assume refractive indices from the OPAC dataset (Hess et al., 1998) and spherical particle shape. In the shortwave (SW) we use mineralogy-based refractive indices and non-spherical (tri-axial spheroid) shapes (Klose et al., 2021). The ARI implementation in MONARCH is based on three main routine fluxes: (I) initialization, (II) calculation of aerosol optical properties per model layer for each step (the optical depth (TAU), the single scattering albedo (SSA) and the asymmetry factor (ASY)), and (III) the effect of aerosols in the radiative fluxes. In the previous operational run the refractive indexes were described by only OPAC climatology and particles were assumed only spherical. With this upgrade we obtain a larger extinction efficiency due to particle asphericity and less absorbing dust particles than the OPAC values, which have been found to be too absorbing (Di Biagio et al., 2019).

Secondly, due to the assumption of spheroid particles there was one important change in the diagnostics of the model. To account for the difference between the geometric and aerodynamic diameter, we consider Huang et al. (2021) with the particulate matter (PM) dust concentrations being now calculated with different equations than before. From

$$PM_{2.5} = \text{bin1} + \text{bin2} + \text{bin3} + \text{bin4} + \text{bin5} * 0.59 \text{ and } PM_{10} = \text{bin1} + \text{bin2} + \text{bin3} + \text{bin4} + \text{bin5} + \text{bin6} + \text{bin7} * 0.96$$

to

$$PM_{2.5} = \text{bin1} + \text{bin2} + \text{bin3} + \text{bin4} * 0.43 \text{ and } PM_{10} = \text{bin1} + \text{bin2} + \text{bin3} + \text{bin4} + \text{bin5} + \text{bin6} + \text{bin7} * 0.31$$

Note: Right now, the BDRC products do not include dust $PM_{2.5}$ and PM_{10} forecasts, but only dust total surface concentration forecasts. However, in this report we evaluate our upgrade using DOD together with $PM_{2.5}$ and PM_{10} concentrations.

1.3. Upgrade in infrastructure

Improvements have also been introduced in the operational workflow and the infrastructure.

Since the first version, the system has been deployed and executed daily on both operational machines of the WMO Barcelona Dust Forecast Center. The two independent runs, performed respectively at the BSC and the AEMET HPC facilities, guarantee redundancy in case of technical failure or maintenance. In July 2021, the AEMET cluster (Nimbus) was replaced by a new one (Cirrus), which implied the installation of the at-the-time operational version of MONARCH in the new cluster and the migration of the auto-MONARCH system, based on the Autosubmit workflow manager, to the new infrastructure. This new cluster has provided better performance and execution times compared to the old one. In the current upgrade, we benefit from the work already done in this migration (deployment of the software stack, installation of external libraries, etc.), and we complement it with improvements in the model and the entire production process. First, a few minor changes were needed to execute the new version of the model on Cirrus, mainly related to the compilation of the model using the GNU compiler (GCC).

The most significant change implemented in the workflow was the replacement of the old postprocessing and diagnostic tools with a single one called SNES. SNES has been recently developed at the BSC and provides almost all the operations needed to postprocess and generate diagnostics from the MONARCH outputs in a single parallelized tool. It can also write the resulting data in the netCDF and Grib formats without using any external tool like CDO. Thus, the inclusion of SNES has brought a huge simplification of the workflow as well as a big improvement in the execution time compared to the previous version, reducing the post-process time by 50%.

The introduction of SNES opens the possibility of integrating the entire post-process phase within the workflow. The production of images displayed on the BDRC website is currently not yet performed by SNES. We are considering introducing it into this tool so that it can be executed directly in the auto-MONARCH workflow and, therefore, take advantage of Autosubmit's failure tolerance by managing automatic retrials in case of failures.

In the end, a summary of the different upgrades from the previous operational model (MONARCH v1.0.0) and the updated one (MONARCH v2.1.0), are summarized in Table 1.1.

Table 1.1 The changes introduced in the operational version of the MONARCH model of the BDRC.

MONARCH Version	Date of deployment	Description of changes
v0.0.0	February 2012	<ul style="list-style-type: none"> ● Pérez et al. (2011) version
v1.0.0	December 2020	<ul style="list-style-type: none"> ● Introduction of different dust source functions ● Introduction of different dust emission sources and emission schemes ● Introduction of developments described in Perez et al. (2011), Spada (2015), Badia et al. (2017) and Di Tomaso (2017).
v2.1.0	June 2023	<ul style="list-style-type: none"> ● Aerosol-radiation interaction allowed with dynamic coupling of dust-radiation ● Introduction of spheroid particles ● SNES tool in the workflow.

2. Evaluation strategy

The assessment of the model results for the different experiments considered in this sensitivity analysis are done comparing the model results against dust optical depth (DOD) observations and particulate matter (PM) concentrations. Standard statistics such as correlation coefficient (COR), mean bias error (MB) and root mean square error (RMSE) are used to measure the skill of the model when performing diagnostic analyses at specific locations.

2.1 Dust optical depth (DOD) observations: the global AERONET network

Dust-filtered AOD observations from AERONET (Aerosol, Robotic NETwork; Holben, 2001: <http://aeronet.gsfc.nasa.gov/>) are used for the assessment of the model results. The dust-filtering considered here is based on the Spectral Deconvolution Algorithm (SDA, also known as O'Neill; O'Neill et al., 2003) AERONET products that provide AODcoarse and AODfine fractions. AODcoarse observations are fundamentally associated with maritime/oceanic aerosols and desert dust. Since sea-salt is related to low AOD (< 0.03 ; Dubovik et al., 2002) and mainly affects coastal stations, high AODcoarse values are mostly related to mineral dust (i.e. DODcoarse). We also compare with the dust-filtered direct-sun total AOD observations. The dust filtering is based on the Angstrom Exponent (where $DOD=AOD$ is considered only when $AE < 0.6$). For the present evaluation exercise, we use the SDA Version 3 cloud-screened (Level 1.5) observations. These observations are used for operational evaluation purposes in the WMO Barcelona Dust Regional Center.

For the comparison, modeled DOD and DODcoarse fields are bilinearly interpolated over the AERONET stations. Because AERONET data are acquired at 15-min intervals, all AERONET measurements within ± 90 min of the 3-hourly instantaneous model outputs have been extracted and averaged to perform a model comparison. All AERONET stations that are available for the year 2021 and are included in the North Africa, Mediterranean and Middle East (NAMEE) domain are used in the evaluation.

2.2 PM₁₀ and PM_{2.5} comparison in Spain

For Spain, we include the comparison of MONARCH with the PM₁₀ and PM_{2.5} dust-filtered observations provided by the CSIC-IDAEA and available through the Spanish government website: (<https://www.miteco.es/es/calidad-y-evaluacion-ambiental/temas/atmosfera-y-calidad-del-aire/calidad-del-aire/evaluacion-datos/fuentes-naturales/default.aspx>). In this case 3-hourly outputs of our model are averaged on daily basis for the comparisons with the CSIC-IDAEA dataset.

3. Results

3.1 Annual comparison

The annual comparison for the derived DOD and DODcoarse from the previous operational model (v1.0.0) and the model upgrade (v2.1.0) are shown in Fig. 3.1, as well as for the dust PM_{10} and $PM_{2.5}$ concentrations for the full NAMEE domain. The main dust sources in Africa are emphasized in both simulations (El Djouf desert and Bodélé Depression). From the differences of the two simulations, it is observed that the previous version has increased values in the North Africa and Middle East for all variables. This is expected due to the more realistic assumption of dust-radiation interaction with spheroid particles that results in a reduction of the extinction efficiency, with less absorbing dust particles. The new upgrade only suggests some increased DOD over the Sahel region for the Southern Part of Algeria (around Tamanrasset), Niger and Chad. The reduction of the surface dust PMs concentrations in North Africa and Middle East is particularly significant (Figure 3.1). This is once again explained by the new assumption of the spheroid particles and the different equation used in the diagnostics for the PM concentrations, accounting for the difference between the geometric and aerodynamic diameter (Huang et al. 2021).

3.2 DOD comparison over NAMEE

The old operational (v.1.0.0) and upgraded (v.2.1.0) MONARCH runs have been compared initially at four selected stations using dust-filtered direct-sun AOD AERONET observations (Version 3 Level 1.5) for the year 2021 (see Figure 3.2) as well as AODcoarse O'Neill (see Figure 3.3). These stations are Banizoumbou in Niger, Tamanrasset in Southern Algeria, KAUST campus in Kuwait and Palma de Mallorca in the Mediterranean Sea. From the direct-sun observations (Figure 3.2) the upgraded MONARCH shows lower annual averages for the stations of Banizoumbou and KAUST campus compared to the previous old operational. This comes to an agreement with the annual evaluation (shown in Figure 3.1), where the old operational had higher total DOD in North Africa and Middle East. The annual averages for the station of Palma de Mallorca are almost the same (0.23 versus 0.24) from the two runs. The annual cycle and the dust events are reproduced with both runs and the correlations are improved in Banizoumbou and Tamanrasset with the upgraded MONARCH. The RMSE and MB are also improved in most cases with the MONARCH upgraded, while only for Palma de Mallorca the correlation is decreased (from 0.73 to 0.69) while the RMSE is the same and the mean bias is slightly increased. From the O'Neill AODcoarse observations (Figure 3.3) now the Tamanrasset station has a higher mean value for the upgraded run compared to the old operational MONARCH, coming again into agreement with the annual comparison (see Figure 3.1), when the annual DODcoarse had increased values over Southern Algeria with the upgraded run. The results once again show improvements in the correlations for all stations except Palma de Mallorca where again the correlation slightly decreased (from 0.75 to 0.72). Same trend had RMSE and MB.

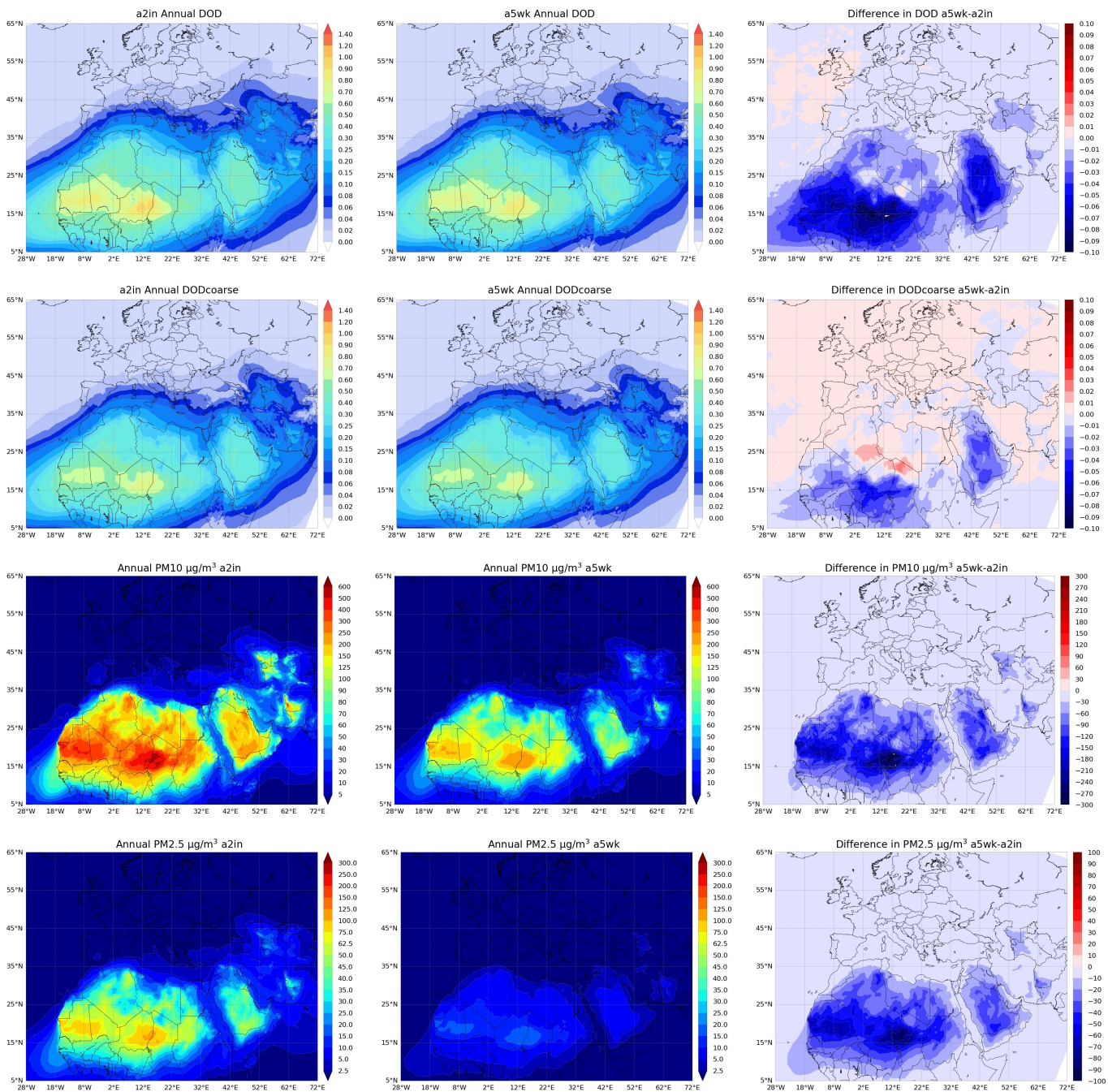


Figure 3.1 Annual DOD, DODcoarse, PM₁₀ and PM_{2.5} for the NAMEE domain for 2021. First is shown the MONARCH v1.0.0 annuals (left columns), second the MONARCH v2.1.0 (central column) and last the difference (MONARCH v2.1.0-MONARCH v1.0.0, right column). The annual calculation is based on the averaging of 3-hourly inputs of the simulations.

The correlations, mean biases (MB) and RMSE for DODcoarse from the models were evaluated for all 94 O'Neill stations for the two runs (see Figure 3.4). For most stations the differences

between the two runs were small with slightly lower RMSE for the upgraded MONARCH mostly in the Middle East and North Africa close to the Atlantic coast. The statistics for both AOD directsun and AODcoarse O'Neill are summarized (see Table 3.1). For AODcoarse O'Neill, the correlations considering all stations were the same and there was a small improvement in the reduction of RMSE. For AOD directsun, the correlation was slightly decreased but the MB and RMSE were reduced. The conclusion is that the upgraded MONARCH with the decreased values of AOD led to a reduction of the overestimations of dust in most cases.

Table 3.1. Statistics performed for the old operational and new upgrade of MONARCH for the study period for AODcoarse measurements of all AERONET stations in the NAMEE region, for PM₁₀ measurements of all CSIC stations in Spain, for AOD directsun (AE<0.6) measurements of all AERONET stations in the NAMEE region and PM_{2.5} measurements of all CSIC stations in Spain. We report the correlation coefficient (r), Mean Bias (MB) and Root Mean Square Error (RMSE).

MONARCH versión	AODcoarse O'Neill/DODcoarse from models			PM10du			AOD directsun/DOD from models			PM2.5du		
	r	MB	RMSE	r	MB	RMSE	r	MB	RMSE	r	MB	RMSE
Old operational	0.74	0.00	0.13	0.50	0.07	30.44	0.55	0.04	0.29	0.22	-1.46	8.08
New upgrade	0.74	0.00	0.12	0.52	-8.67	22.8	0.54	0.02	0.27	0.18	-4.92	7.91

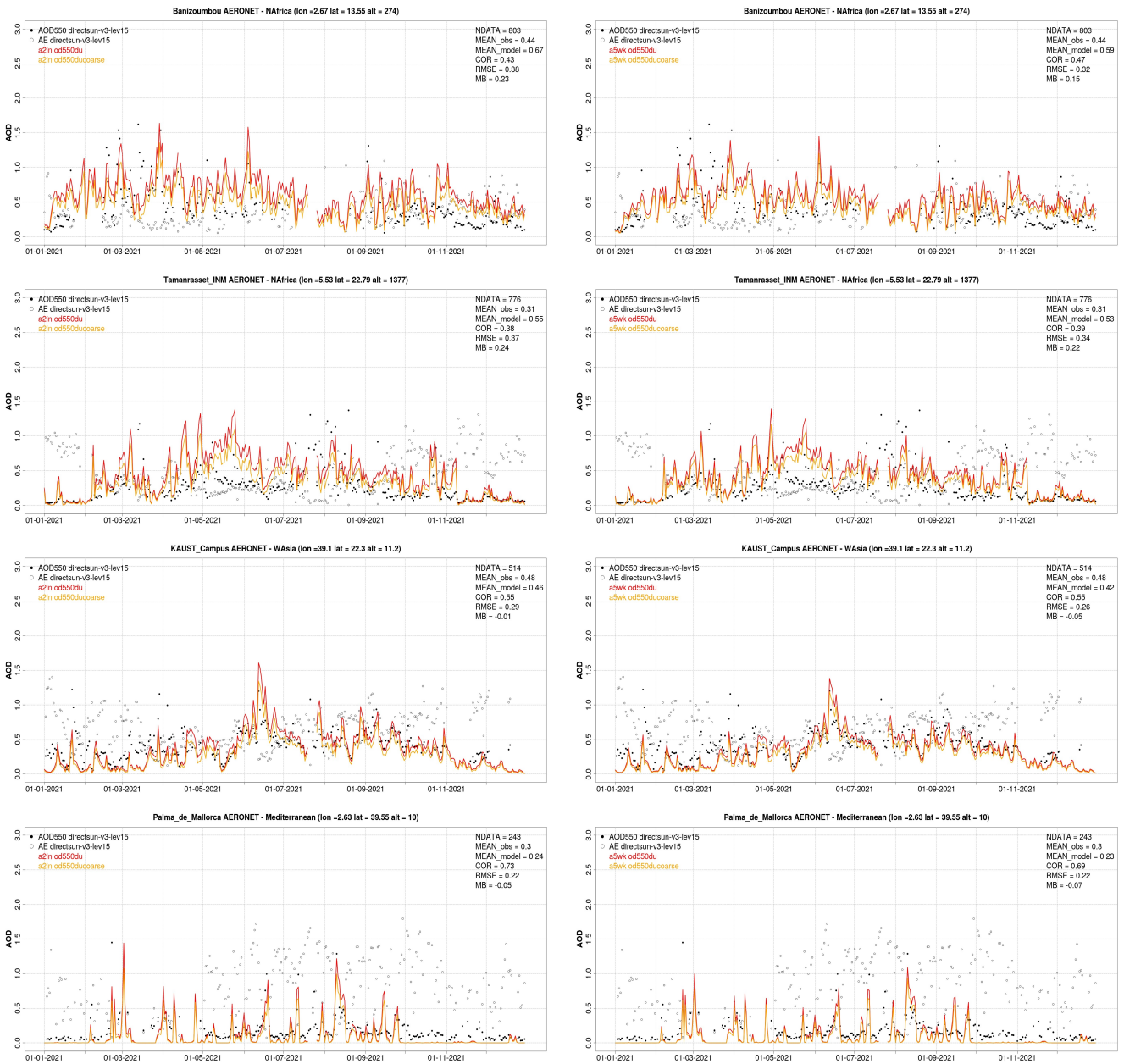


Figure 3.2 AOD and Angstrom Exponent (AE) from AERONET Direct-sun (black dots and white circles), DOD MONARCH (red line) and DODcoarse MONARCH (orange line) for 2021 over Banizoumbou (first row), Tamanrasset (second row), KAUST campus (third row) and Palma de Mallorca (fourth row). Left column: MONARCH v1.0.0. Right column: MONARCH v2.1.0. Skill scores per site and model are shown in the upper right corner (NDATA: 3-hourly pairs used for the calculations of the statistics, MEAN observations, MEAN model, correlation, RMSE, MB). The AE has the same axis units as AOD.

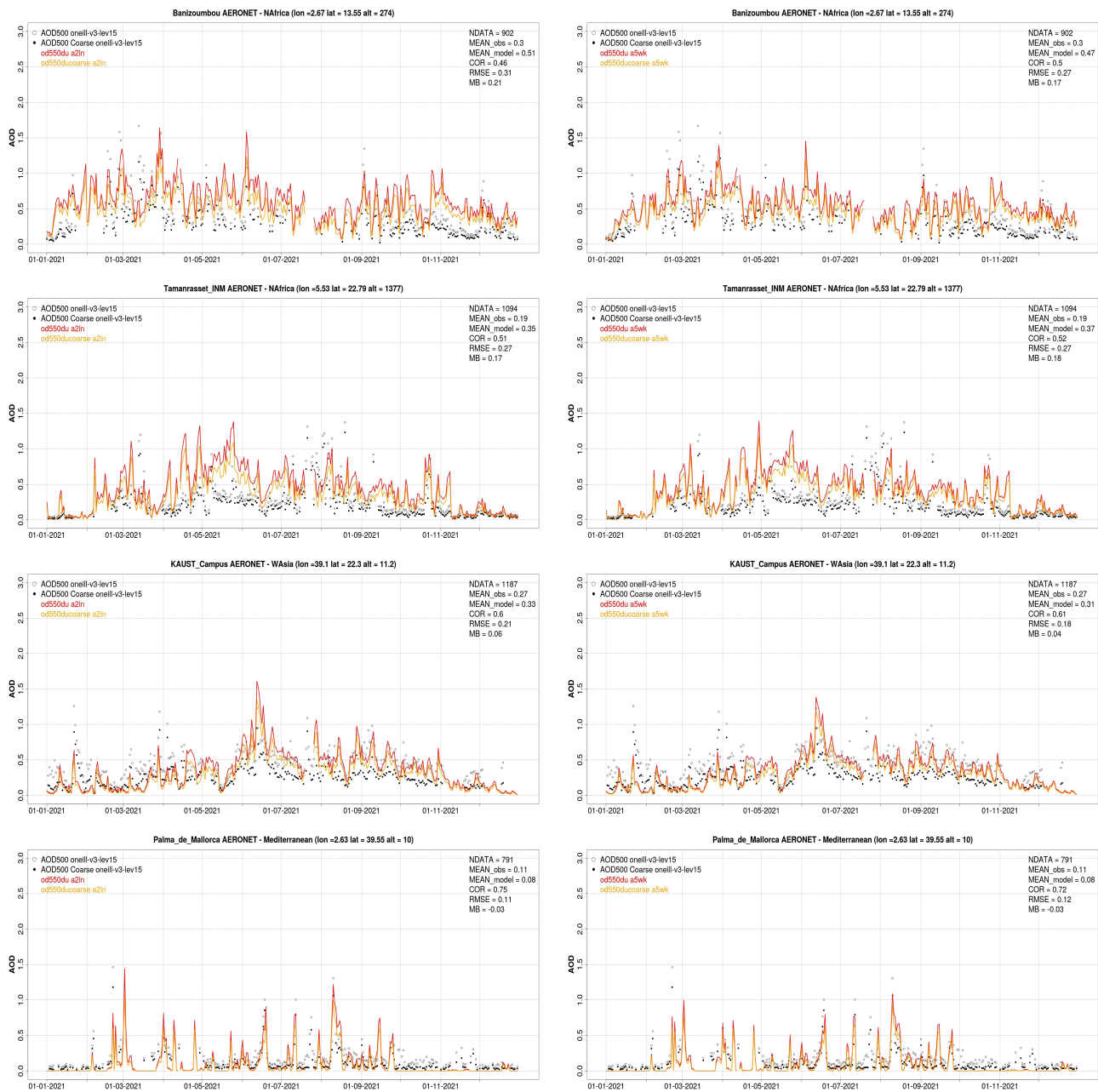


Figure 3.3 AOD and AODcoarse O'Neill from SDA AERONET (white circles, black dots), DOD MONARCH (red line) and DODcoarse MONARCH (orange line) for 2021 over Banizoumbou (first row), Tamanrasset (second row), KAUST campus (third row) and Palma de Mallorca (fourth row). Left column: MONARCH v1.0.0. Right column: MONARCH v2.1.0. Skill scores per site and model are shown in the upper right corner (NDATA: 3-hourly pairs used for the calculations of the statistics, MEAN observations, MEAN model, correlation, RMSE, MB).

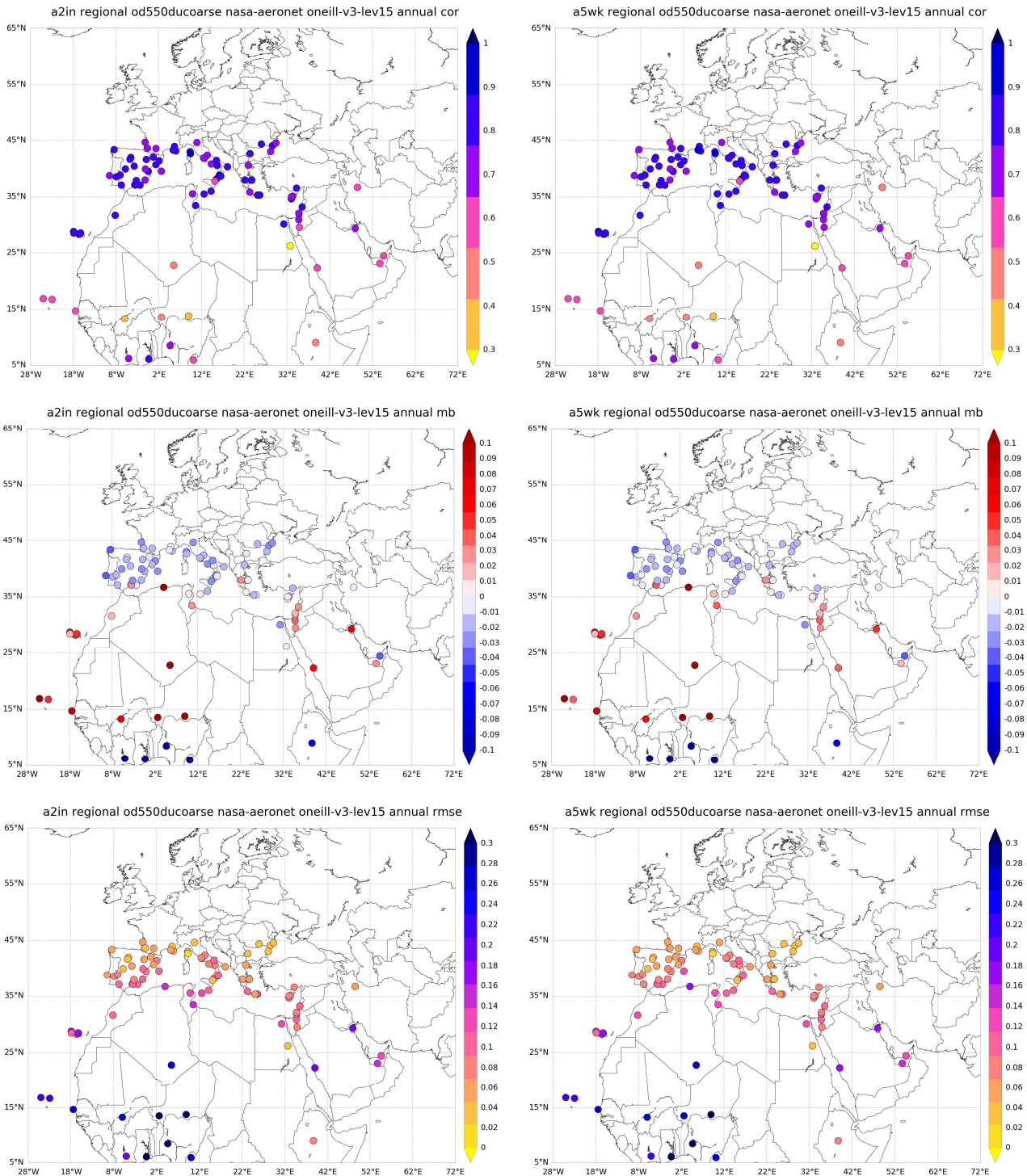


Figure 3.4 Skill scores as the correlation (first row), MB (second row) and RMSE (third row) for AODcoarse SDA O'Neill for 2021. Left column: MONARCH v1.0.0. Right column: MONARCH v2.1.0.

3.3 Dust PM_{10} and $PM_{2.5}$ comparison in Spain

The old operational and upgraded MONARCH runs have been compared with PM_{10} and $PM_{2.5}$ dust-filtered observations in Spain provided by the CSIC-IDAIA. Both MONARCH runs can reproduce the observed daily PM_{10} dust variability, as in Viznar, Granada (see Figure 3.5), El

Atazar, Madrid (see Figure 3.6) and Tefía of Puerto del Rosario, Las Palmas (see Figure 3.7) for 2021.

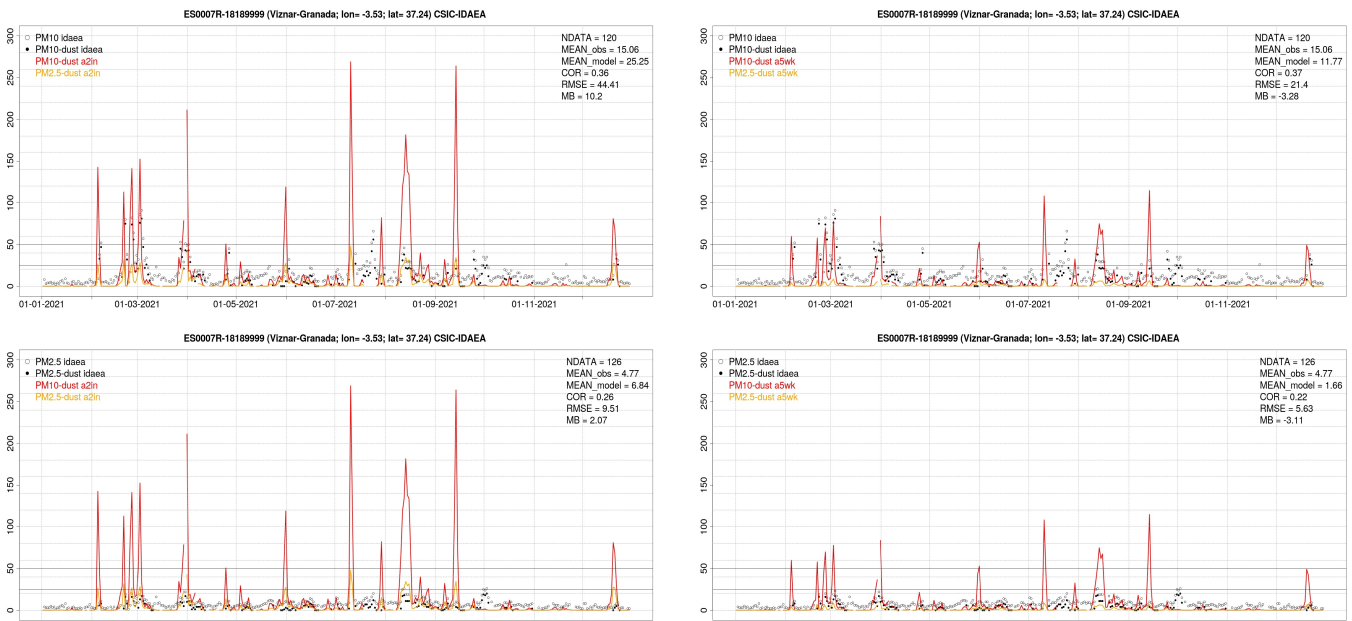


Figure 3.5 Daily PM time series. PM_{10} (first row), $PM_{2.5}$ (second row), PM from CSIC-IDAEA (white circles, all aerosols), PM-dust from CSIC-IDAEA (black dots), PM_{10} -dust MONARCH (red line) and $PM_{2.5}$ -dust MONARCH (orange line) for 2021 over Viznar, Granada. Left column: MONARCH v1.0.0. Right column: MONARCH v2.1.0. Skill scores per site and model are shown in the upper right corner (NDATA: available days, MEAN observations, MEAN model, correlation, RMSE, MB). Daily averages from the model are calculated using a 3-hourly dataset. Some days with missing model values in one of the two simulations have been excluded from both datasets.

Correlations are improved in most cases with the upgraded MONARCH while the lower predicted PM concentrations, as they were discussed earlier also (see Figure 3.1), seem to smooth some extreme PM_{10} peaks that appeared in the operational MONARCH version. In Viznar, Granada for PM_{10} the MB and RMSE are also half for the upgraded MONARCH, while in El Atazar, Madrid the lower prediction with the upgraded MONARCH leads to lower RMSE (by 15%) and higher MB (from -4 to $-15 \mu\text{g m}^{-3}$ approximately). In Madrid, the upgraded model underpredicts the strength of the dust events (with lower peaks). In the Canarias (Figure 3.7) there are some very high overpredictions of the peaks with the old operational while the new upgrade has peaks closer to the measurements. Also, once again the RMSE is reduced (from 48 to $42 \mu\text{g m}^{-3}$) while MB is increased (from -1 to $-17 \mu\text{g m}^{-3}$). For $PM_{2.5}$ concentrations the correlation for the two stations of Granada and Madrid (there are no observations for $PM_{2.5}$ in Tefía of Puerto del Rosario) is lower for both models and in Granada the RMSE is less with the

upgraded MONARCH while in Madrid it is the opposite, and the MB is higher.

The same conclusions appear for most of the 22 stations used in this analysis for the PM₁₀ concentrations (see Figure 3.8). The annual correlation coefficients are between 0.4 and 0.5 considering most of the stations with higher values (0.7-0.8) at the Canary stations. The mean biases are increased, mostly because the upgraded MONARCH smooths out the high dust peaks observed in most stations. The RMSE is decreased with the upgraded MONARCH also in many stations of the Iberian Peninsula. In terms of annual statistics (Table 3.1) the correlation for PM₁₀ concentrations is improved with the upgraded MONARCH, while the RMSE reduces as well (30.4 to 22.4 $\mu\text{g m}^{-3}$). The MB is increased because of the lower estimations for PM concentrations with the upgraded MONARCH. For PM_{2.5} the old operational model shows better statistics for correlation and MB and the upgraded MONARCH has lower RMSE.

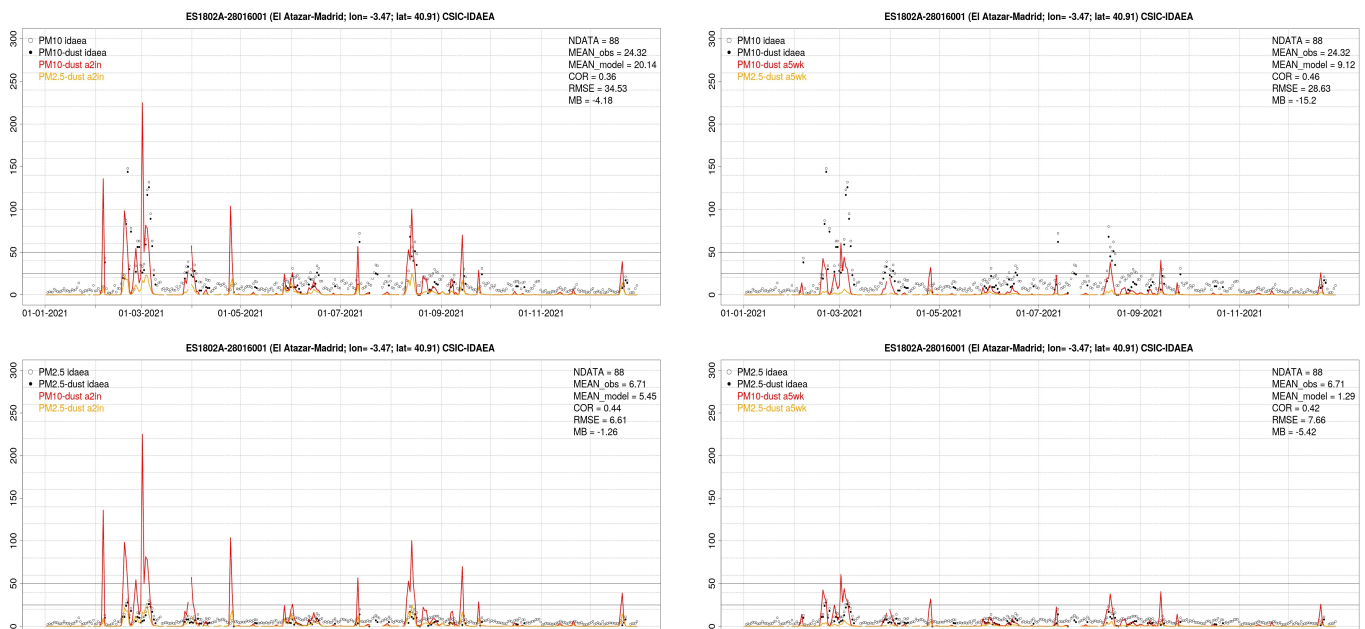


Figure 3.6 Daily PM time series ($\mu\text{g m}^{-3}$). PM₁₀ (first row), PM_{2.5} (second row), PM from CSIC-IDAEA (white circles, all aerosols), PM-dust from CSIC-IDAEA (black dots), PM₁₀-dust MONARCH (red line) and PM_{2.5}-dust MONARCH (orange line) for 2021 over El Atazar, Madrid. Left column: MONARCH v1.0.0. Right column: MONARCH v2.1.0. Skill scores per site and model are shown in the upper right corner (NDATA: available days, MEAN observations, MEAN model, correlation, RMSE, MB). Daily averages from the model are calculated using a 3-hourly dataset. Some days with missing model values in one of the two simulations have been excluded from both datasets.

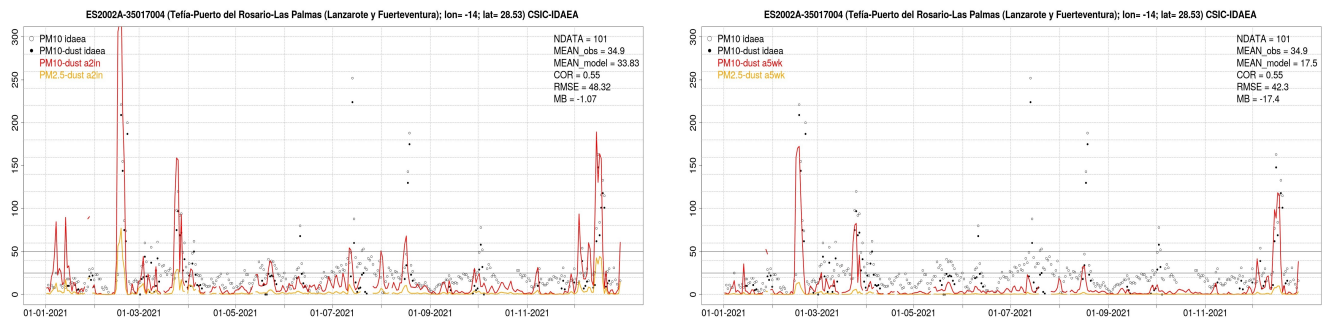


Figure 3.7 Daily PM_{10} time series ($\mu\text{g m}^{-3}$). PM_{10} from CSIC-IDAEA (white circles, all aerosols and only dust with black dots), PM_{10} -dust MONARCH (red line) and $PM_{2.5}$ -dust MONARCH (orange line) for 2021 over Tefía of Puerto del Rosario, Las Palmas. Left column: MONARCH v1.0.0. Right column: MONARCH v2.1.0. Skill scores per site and model are shown in the upper right corner (NDATA: available days, MEAN observations, MEAN model, COR, RMSE, MB). Daily averages from the model are calculated using a 3-hourly dataset. Some days with missing model values in one of the two simulations have been excluded from both datasets.

Finally, we constructed a contingency table to evaluate the two forecasts based on the percentages of times they exceed or not the daily threshold of PM_{10} equal to $50 \mu\text{g m}^{-3}$. As it was suggested from Figure 3.6, for the station of El Atazar, Madrid, the new upgrade shows an average decrease of hit rate (from 37.1% to 17.5%). On the other hand, the new upgrade has a decrease of false alarm rate from about 7% to 1% (Table 3.2).

Overall, the comparison with CSIC-IDAEA observations shows how the upgraded version of the model presents some improved skills scores (i.e. annual correlation coefficient increases and RMSE decreases) with respect to the current operational configuration. The improvement in the false alarms rate comes, however, with a reduction in the hits rates and an increase in the miss rates. The difficulties to match the absolute values of dust PMs concentration during the peaks suggests that some further scientific investigation is needed before considering such product for public dissemination.

Table 3.2. Hit rate and false alarm rate for dust PM₁₀ measurements of all CSIC stations in Spain, based on a threshold daily dust PM₁₀ exceedance of 50 µg m⁻³.

	Hit rate	False alarm rate
MONARCH v1.0.0	37.1%	6.8%
MONARCH v2.1.0	17.5%	1.4%

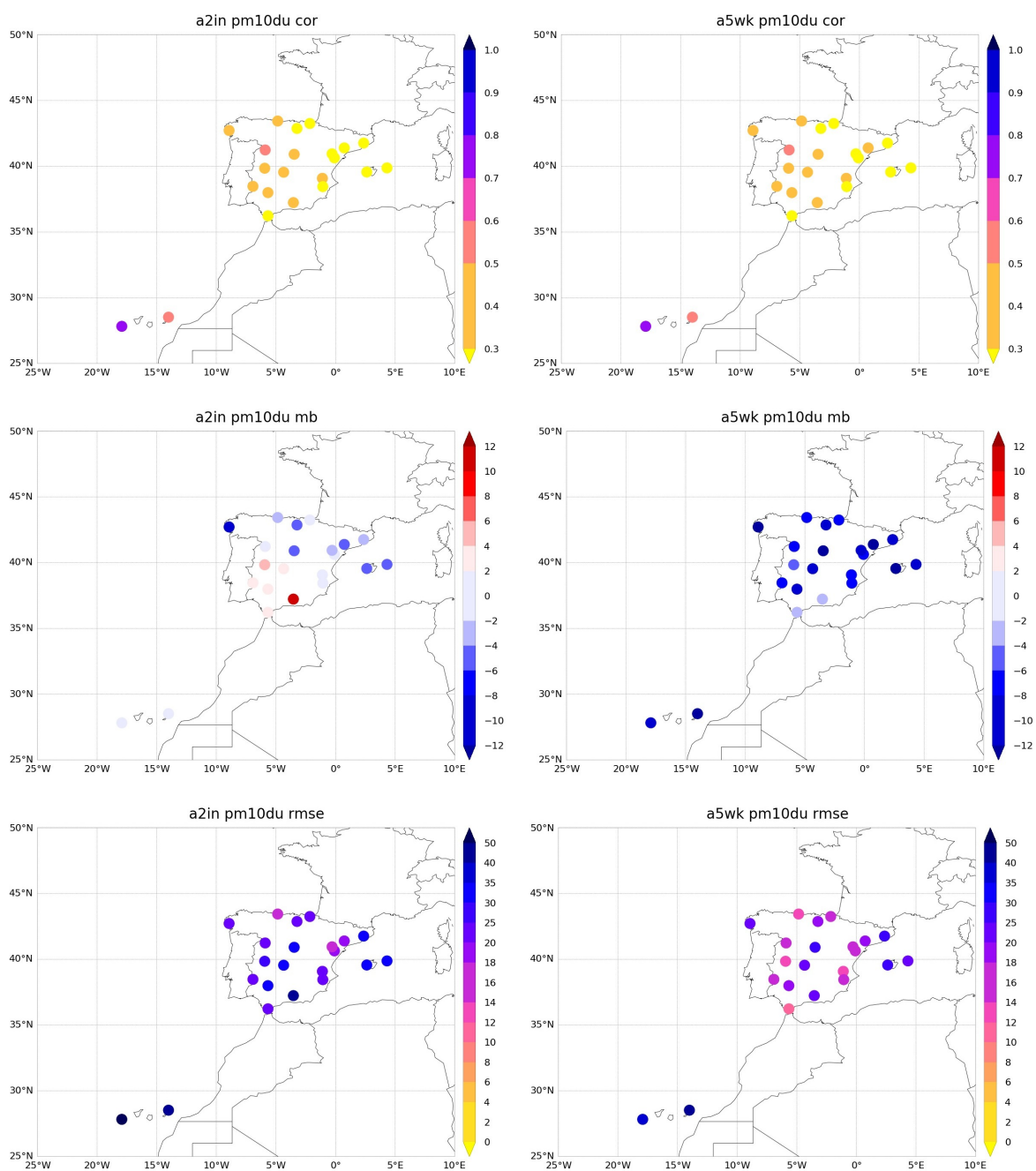


Figure 3.8 Skill scores (correlation coefficient, MB and RMSE) for 24-hour forecasts of daily PM₁₀ MONARCH v1.0.0 (left column), PM₁₀ MONARCH v2.1.0 (right column) for 2021. PM₁₀-dust from CSIC-IDAEA is the reference. Daily averages from the model are calculated using a 3-hourly dataset. Units are in $\mu\text{g m}^{-3}$ for MB and RMSE.

4. Conclusions

MONARCH latest upgrade (**MONARCH v2.1.0**) improved the dust-radiation interaction and introduced the spheroid dust particles together with corrections in the diagnostics of the model concerning the aerodynamic diameter and affecting the particulate matter concentration calculation. The simulations showed less overpredictions of dust for the NAMEE domain and improvements for AOD and PM concentrations with lower RMSE. Thus, **MONARCH was upgraded on 15th of June** with the new changes discussed in this report.

5. References

- Badia, A., & Jorba, O.: Gas-phase evaluation of the online NMMB/BSC-CTM model over Europe for 2010 in the framework of the AQMEII-Phase2 project. *Atmospheric Environment*, 115, 657-669, 2015.
- Badia, A., Jorba, O., Voulgarakis, A., Dabdub, D., Pérez García-Pando, C., Hilboll, A., Gonçalves, M., and Janjic, Z.: Description and evaluation of the Multiscale Online Nonhydrostatic Atmosphere Chemistry model (NMMB-MONARCH) version 1.0: gas-phase chemistry at global scale, *Geosci. Model Dev.*, 10, 609-638, <https://doi.org/10.5194/gmd-10-609-2017>, 2017.
- Di Biagio, C., Formenti, P., Balkanski, Y., Caponi, L., Cazaunau, M., Pangui, E., Journet, E., Nowak, S., Andreae, M. O., Kandler, K., Saeed, T., Piketh, S., Seibert, D., Williams, E., and Doussin, J.-F.: Complex refractive indices and single-scattering albedo of global dust aerosols in the shortwave spectrum and relationship to size and iron content, *Atmos. Chem. Phys.*, 19, 15503-15531, <https://doi.org/10.5194/acp-19-15503-2019>, 2019.
- Di Tomaso, E., Schutgens, N. A. J., Jorba, O., and Pérez García-Pando, C.: Assimilation of MODIS Dark Target and Deep Blue observations in the dust aerosol component of NMMB/BSC-CTM version 1.0. *Geosci. Model Dev.*, 10, 1107-1129, <https://doi.org/10.5194/gmd-10-1107-2017>, 2017.
- Di Tomaso, E., Escribano, J., Basart, S., Ginoux, P., Macchia, F., Barnaba, F., Benincasa, F., Bretonnière, P.-A., Buñuel, A., Castrillo, M., Cuevas, E., Formenti, P., Gonçalves, M., Jorba, O., Klose, M., Mona, L., Montané Pinto, G., Mytilinaios, M., Obiso, V., Olid, M., Schutgens, N., Votsis, A., Werner, E., and Pérez García-Pando, C.: The MONARCH high-resolution reanalysis of desert dust aerosol over Northern Africa, the Middle East and Europe (2007-2016), *Earth Syst. Sci. Data*, 14, 2785-2816, <https://doi.org/10.5194/essd-14-2785-2022>, 2022.
- Dubovik, O., Holben, B., Eck, T. F., Smirnov, A., Kaufman, Y. J., King, M. D., ... & Slutsker, I.: Variability of absorption and optical properties of key aerosol types observed in worldwide locations. *Journal of the atmospheric sciences*, 59(3), 590-608, 2002.
- Escribano, J., Di Tomaso, E., Jorba, O., Klose, M., Gonçalves Ageitos, M., Macchia, F., Amiridis, V., Baars, H., Marinou, E., Proestakis, E., Urbanneck, C., Althausen, D., Bühl, J., Mamouri, R.-E., and Pérez García-Pando, C.: Assimilating spaceborne lidar

- dust extinction can improve dust forecasts, *Atmos. Chem. Phys.*, 22, 535-560, <https://doi.org/10.5194/acp-22-535-2022>, 2022.
- Ginoux, P., Chin, M., Tegen, I., Prospero, J. M., Holben, B., Dubovik, O., & Lin, S. J.: Sources and distributions of dust aerosols simulated with the GOCART model. *Journal of Geophysical Research: Atmospheres*, 106(D17), 20255-20273, 2001.
- Ginoux, P., Prospero, J.M., Gill, T.E., Hsu, N.C., and Zhao, M.: Global-Scale Attribution of Anthropogenic and Natural Dust Sources and Their Emission Rates Based on Modis Deep Blue Aerosol Products, *Rev. Geophys.*, 50, <https://doi.org/10.1029/2012RG000388>, 2012.
- Haustein, K., Pérez, C., Baldasano, J. M., Jorba, O., Basart, S., Miller, R. L., Janjic, Z., Black, T., Nickovic, S., Todd, M. C., Washington, R., Müller, D., Tesche, M., Weinzierl, B., Esselborn, M., and Schladitz, A.: Atmospheric dust modeling from meso to global scales with the online NMMB/BSC-Dust model - Part 2: Experimental campaigns in Northern Africa, *Atmos. Chem. Phys.*, 12, 2933-2958, <https://doi.org/10.5194/acp-12-2933-2012>, 2012.
- Hess, M., Koepke, P., and Schult, I.: Optical properties of aerosols and clouds: The software package OPAC, *B. Am. Meteorol. Soc.*, 79, 831-844, [https://doi.org/10.1175/1520-0477\(1998\)079<0831:OPOAAC>2.0.CO;2](https://doi.org/10.1175/1520-0477(1998)079<0831:OPOAAC>2.0.CO;2), 1998
- Holben, B. N., Eck, T. F., Slutsker, I., Tanré, D., Buis, J. P., Setzer, A., Vermote, E., Reagan, J. A., Kaufman, Y. J., Nakajima, T., Lavenu, F., Jankowiak, I., and Smirnov, A.: AERONET - A federated instrument network and data archive for aerosol characterization, *Remote Sens. Environ.*, 66, 1-16, [https://doi.org/10.1016/S0034-4257\(98\)00031-5](https://doi.org/10.1016/S0034-4257(98)00031-5), 1998.
- Huang, Y., Adebiyi, A. A., Formenti, P., & Kok, J. F.: Linking the different diameter types of aspherical desert dust indicates that models underestimate coarse dust emission. *Geophysical Research Letters*, 48, e2020GL092054, <https://doi.org/10.1029/2020GL092054>, 2021.
- Iacono, M. J., Delamere, J. S., Mlawer, E. J., and Shephard, M. W.: Radiative forcing by long-lived greenhouse gases: Calculations with the AER radiative transfer models, *J. Geophys. Res.-Atmos.*, 113, D13103, <https://doi.org/10.1029/2008JD009944>, 2008.
- Janjic, Z., & Gall, L.: Scientific documentation of the NCEP nonhydrostatic multiscale model on the B grid (NMMB). Part 1 Dynamics, 2012.
- Jorba, O., Dabdub, D., Blaszcak-Boxe, C., Pérez, C., Janjic, Z., Baldasano, J. M., Spada, M., Badia, A., and Gonçalves, M.: Potential significance of photoexcited NO₂ on global air

- quality with the NMMB/BSC chemical transport model, *Journal of Geophysical Research: Atmospheres*, 117, <https://doi.org/10.1029/2012JD017730>, 2012.
- Klose, M., Jorba, O., Gonçalves Ageitos, M., Escribano, J., Dawson, M. L., Obiso, V., Di Tomaso, E., Basart, S., Montané Pinto, G., Macchia, F., Ginoux, P., Guerschman, J., Prigent, C., Huang, Y., Kok, J. F., Miller, R. L., and Pérez García-Pando, C.: Mineral dust cycle in the Multiscale Online Nonhydrostatic Atmosphere Chemistry model (MONARCH) version 2.0, *Geoscientific Model Development*, 14, 6403-6444, <https://doi.org/10.5194/gmd-14-6403-2021>, 2021.
- Kok, J. F., Mahowald, N. M., Fratini, G., Gillies, J. A., Ishizuka, M., Leys, J. F., Mikami, M., Park, M.-S., Park, S.-U., Van Pelt, R. S., and Zobeck, T. M.: An improved dust emission model - Part 1: Model description and comparison against measurements, *Atmos. Chem. Phys.*, 14, 13023-13041, <https://doi.org/10.5194/acp-14-13023-2014>, 2014.
- O'Neill, N. T., Eck, T. F., Smirnov, A., Holben, B. N., & Thulasiraman, S.: Spectral discrimination of coarse and fine mode optical depth. *Journal of Geophysical Research: Atmospheres*, 108(D17), 2003.
- Pérez, C., Nickovic, S., Pejanovic, G., Baldasano, J. M., & Özsoy, E.: Interactive dust-radiation modeling: A step to improve weather forecasts. *Journal of Geophysical Research: Atmospheres*, 111(D16), 2006.
- Pérez, C., Haustein, K., Janjic, Z., Jorba, O., Huneus, N., Baldasano, J. M., Black, T., Basart, S., Nickovic, S., Miller, R. L., Perlwitz, J. P., Schulz, M., and Thomson, M.: Atmospheric dust modeling from meso to global scales with the online NMMB/BSC-Dust model - Part 1: Model description, annual simulations and evaluation, *Atmos. Chem. Phys.*, 11, 13001-13027, <https://doi.org/10.5194/acp-11-13001-2011>, 2011.
- Spada, M., Jorba, O., Pérez García-Pando, C., Janjic, Z., & Baldasano, J. M.: Modeling and evaluation of the global sea-salt aerosol distribution: sensitivity to size-resolved and sea-surface temperature dependent emission schemes. *Atmospheric Chemistry and Physics*, 13(23), 11735-11755m, 2013.
- Spada, M.: Development and evaluation of an atmospheric aerosol module implemented within the NMMB/BSC-CTM, 2015.
- Xian, P., Reid, J. S., Hyer, E. J., Sampson, C. R., Rubin, J. I., Ades, M., Asencio, N., Basart, S., Benedetti, A., Bhattacharjee, P. S., Brooks, M. E., Colarco, P. R., da Silva, A. M., Eck, T. F., Guth, J., Jorba, O., Kouznetsov, R., Kipling, Z., Sofiev, M., Pérez García-Pando, C., Pradhan, Y., Tanaka, T., Wang, J., Westphal, D. L., Yumimoto, K., and Zhang, J.: Current state of the global operational aerosol multi-model ensemble: An

update from the International Cooperative for Aerosol Prediction (ICAP), *Q. J. Roy. Meteor. Soc.*, 145, 176-209, <https://doi.org/10.1002/qj.3497>, 2019.

Zhang, L., Gong, S., Padro, J., and Barrie, L.: A size-segregated particle dry deposition scheme for an atmospheric aerosol module, *Atmos. Environ.*, 35, 549-560, [https://doi.org/10.1016/S1352-2310\(00\)00326-5](https://doi.org/10.1016/S1352-2310(00)00326-5), 2001.